

Measurement of the Nuclear Modification Factor and Prompt Charged Particle Production in p -Pb and pp Collisions at $\sqrt{s_{NN}} = 5$ TeV

R. Aaij *et al.*^{*}
(LHCb Collaboration)



(Received 31 August 2021; accepted 14 February 2022; published 7 April 2022)

The production of prompt charged particles in proton-lead collisions and in proton-proton collisions at the nucleon-nucleon center-of-mass energy $\sqrt{s_{NN}} = 5$ TeV is studied at LHCb as a function of pseudorapidity (η) and transverse momentum (p_T) with respect to the proton beam direction. The nuclear modification factor for charged particles is determined as a function of η between $-4.8 < \eta < -2.5$ (backward region) and $2.0 < \eta < 4.8$ (forward region), and p_T between $0.2 < p_T < 8.0$ GeV/ c . The results show a suppression of charged particle production in proton-lead collisions relative to proton-proton collisions in the forward region and an enhancement in the backward region for p_T larger than 1.5 GeV/ c . This measurement constrains nuclear PDFs and saturation models at previously unexplored values of the parton momentum fraction down to 10^{-6} .

DOI: 10.1103/PhysRevLett.128.142004

Charged particle production in hadronic collisions is a fundamental observable for studying the properties of the strong interaction governed by quantum chromodynamics (QCD). In high-energy collisions at the Large Hadron Collider (LHC), charged particles can be produced in soft and hard interactions which correspond to small and large momentum exchanges between the interacting partons of the hadrons, respectively. While hard interactions can be described by perturbative QCD (PQCD), the soft regime is less well understood and predictions currently rely on phenomenological considerations [1,2]. Even at LHC energies, charged particles from soft interactions dominate over those from hard interactions. For this reason, experimental input is crucial to improve models and generators for hadron collider and cosmic ray physics [3–5].

The study of the hard regime, which corresponds to charged particles of high transverse momentum (p_T) with respect to the axis of the colliding hadrons, provides valuable information on the physics of heavy-ion collisions [6]. Modifications of the charged particle production rate in proton-lead (p -Pb) collisions relative to proton-proton (pp) collisions can be modeled assuming a variety of cold nuclear matter (CNM) effects [7,8]. Recent indications of collective fluidlike phenomena in small systems suggest the presence of dynamics not generally classified as CNM effects but as signatures of a quark gluon plasma [9].

For charged particles, these modifications are generally associated with initial-state effects, parameterized in nuclear parton distribution functions (NPDFs) [10–12]. Other nuclear effects are related to initial- or final-state multiple scatterings of incoming and outgoing partons [13,14], and could manifest in a Cronin enhancement [15]. Another approach considers models based on parton saturation, an effect arising at low values of the parton momentum fraction, x , and heavy nuclei [16]. In this regime, the QCD dynamics can be described by the color glass condensate (CGC) effective field theory [17]. Pion production at central rapidity [18] is well described by modified NPDFs, energy loss, and CGC calculations [10,11,19,20]. Low values of x , where saturation effects are most likely to occur, can be probed with high-energy collisions at the most forward rapidities.

Previous studies at the LHC [21–23] have measured prompt charged particle production in p -Pb collisions at the center-of-mass energy in the nucleon-nucleon system $\sqrt{s_{NN}} = 5$ TeV in the central pseudorapidity region. At the Relativistic Heavy Ion Collider (RHIC), measurements with deuteron-gold and proton-gold (p -Au) collisions at more forward rapidities but lower energy ($\sqrt{s_{NN}} = 200$ GeV) have been performed [24–26]. The LHCb experiment can uniquely probe the lowest x ranges currently accessible, given its forward rapidity coverage and higher collision energy.

This Letter presents the measurement of the prompt charged particle spectra in p -Pb and pp collisions at $\sqrt{s_{NN}} = 5$ TeV in the $0.2 < p_T < 8.0$ GeV/ c range, thus covering the soft and hard production regimes. The p -Pb measurement covers the backward pseudorapidity range of $-5.2 < \eta < -2.5$, where the lead beam enters the LHCb

*Full author list given at the end of the article.

Published by the American Physical Society under the terms of the Creative Commons Attribution 4.0 International license. Further distribution of this work must maintain attribution to the author(s) and the published article's title, journal citation, and DOI. Funded by SCOAP³.

spectrometer at the interaction point, and the *forward* pseudorapidity range of $1.6 < \eta < 4.3$, where the proton beam enters the LHCb spectrometer at the interaction point. The pp measurement spans over $2.0 < \eta < 4.8$, and complements the recent measurement of prompt charged particle production at $\sqrt{s_{NN}} = 13$ TeV [27]. Throughout the text η is expressed in the nucleon-nucleon center-of-mass system, and is related with the pseudorapidity in the laboratory frame η_{lab} by $\eta = \eta_{\text{lab}} - 0.465$ for $p\text{-Pb}$ and $\eta = \eta_{\text{lab}}$ for pp collisions.

The double-differential production cross section for prompt charged particles is measured as

$$\frac{d^2\sigma^{\text{ch}}(\eta, p_T)}{dp_T d\eta} \equiv \frac{1}{\mathcal{L}} \frac{N^{\text{ch}}(\eta, p_T)}{\Delta p_T \Delta \eta}. \quad (1)$$

Here, N^{ch} is the number of prompt charged particles produced in a given interval of η and p_T , $\Delta\eta$, and Δp_T , respectively, and \mathcal{L} is the integrated luminosity of the corresponding data sample. In this study a prompt charged particle is any charged hadron or lepton with a mean lifetime above 0.3×10^{-10} s produced directly in the collision or from decays of shorter-lifetime particles [28]. The nuclear modification factor, $R_{p\text{Pb}}$, is defined as

$$R_{p\text{Pb}}(\eta, p_T) \equiv \frac{1}{A} \frac{d^2\sigma_{p\text{Pb}}^{\text{ch}}(\eta, p_T)/dp_T d\eta}{d^2\sigma_{pp}^{\text{ch}}(\eta, p_T)/dp_T d\eta}, \quad (2)$$

where $A = 208$ is the number of nucleons in the lead ion and $d^2\sigma_{p\text{Pb}, pp}^{\text{ch}}(\eta, p_T)/dp_T d\eta$ is the double-differential cross section in $p\text{-Pb}$ and pp collisions, respectively.

The LHCb detector is a single-arm forward spectrometer described in Refs. [29,30]. The detector elements that are particularly relevant to this analysis are a silicon-strip vertex detector (VELO) surrounding the interaction region that allows the determination of the position of the collision point, known as the primary vertex (PV), a tracking system that provides a measurement of the momentum, p , of charged particles and two ring-imaging Cherenkov detectors that are able to discriminate between different species of charged particles.

The corresponding integrated luminosity for the forward (backward) $p\text{-Pb}$ data sample is $42.7 \pm 1.0 \mu\text{b}^{-1}$ ($38.7 \pm 1.0 \mu\text{b}^{-1}$) [31], where the uncertainties are uncorrelated between the two data samples. Events are required to pass a minimum-bias trigger which requires at least one reconstructed track in the VELO detector. Additionally, only events with one reconstructed PV within 3 standard deviations from the mean PV position of the full sample are considered.

The pp data correspond to an integrated luminosity of $3.49 \pm 0.07 \text{ nb}^{-1}$. An unbiased trigger for pp events is used to select every leading bunch crossing that occurred

during the data taking period, thus avoiding potential contamination between neighboring bunches.

Simulation is used to model the reconstruction efficiency, the effects of the selection requirements, and the contribution from background tracks. In the simulation, $p\text{-Pb}$ collisions are generated using EPOS LHC [32], while pp collisions are generated using PYTHIA [33] with a specific LHCb configuration [34]. Particle decays are described by EVTGEN [35], while the interaction of particles with the detector, and its response in simulation, are implemented using the GEANT4 toolkit [36,37] as described in Ref. [38].

Prompt charged particle candidates are defined as tracks with hits in the VELO and the tracking stations after the LHCb detector dipole. This last condition requires the measured particle to have $p > 2 \text{ GeV}/c$. Background contributions due to fake tracks and secondary particles are considered in this study. Fake tracks are reconstruction artifacts that do not correspond to actual charged particles, which are particularly relevant for large detector occupancies and in the high- p_T region. Secondary particles are tracks produced by charged particles that do not meet the prompt particle definition and originate from interactions of particles with the detector material or from decays of prompt particles.

A selection is applied to reduce these background contributions. Fake tracks are suppressed with a tight requirement on the output of a neural-net based algorithm (ghost probability) [39]. To suppress further the fake track background, when two or more candidates from the same event share a segment reconstructed in the VELO, only the candidate with the best track fit quality is retained. Secondary particles are reduced by requiring small impact parameters with respect to the mean of the PV distribution in the full sample. This criterion is particularly effective at removing hadrons produced in decays of prompt K_S^0 and Λ particles and in interactions of hadrons with the detector material without inducing a bias by requiring a PV.

The prompt charged particle yield, N^{ch} , for the $p\text{-Pb}$ and pp samples is obtained from the number of candidates, which is corrected with the reconstruction efficiency, the selection efficiency, and the signal purity. The reconstruction efficiency accounts for detector inefficiencies or acceptance effects. The track-finding efficiency from simulation is corrected with a tag-and-probe method applied to data and simulation in two-dimensional intervals of η_{lab} and p_T using $J/\psi \rightarrow \mu^+ \mu^-$ decays in the range $5 < p < 200 \text{ GeV}/c$ [40]. Since the reconstruction efficiency depends on the detector occupancy, the simulated samples are weighted to reproduce the occupancy distributions from different LHCb subdetectors in data. Additionally, the reconstruction efficiency depends on the particle type. The relative abundance of particles determined from simulation are validated with data from the ALICE [41–44] and LHCb [45] experiments. The LHCb PYTHIA tune for pp

collisions does not reproduce the kaon and prompt hyperons relative abundance at high p_T in data. Therefore, a dedicated simulated sample generated with EPOS-LHC [32] is used to parameterize the particle composition in pp collisions. The relative abundances produced with the EPOS-LHC generator are in agreement with the data within 30% in pp and $p\text{-Pb}$ collisions. As a cross-check, the relative abundances from EPOS-LHC in the LHCb acceptance are found to be compatible with those produced with PYTHIA using the rope hadronization model [46,47]. The use of the uncorrected LHCb PYTHIA tune would imply an overestimation of the reconstruction efficiency up to a 7% at high p_T .

The selection efficiency accounts for the fraction of prompt charged particles removed from the candidate sample by the selection. The efficiency is estimated using simulation and a dedicated calibration procedure using a tag-and-probe technique applied to $\phi(1020) \rightarrow K^+K^-$ decays in data and simulation.

The signal purity is determined in simulation and corrected with background-enriched samples of data. Two independent samples dominated by fake tracks are constructed: using tracks with high ghost probability, and tracks which share their reconstructed VELO segment with a better fit-quality track. For secondary particles, the contributions from hadrons and electrons are studied separately. An enriched sample of hadrons from prompt-particle decays, such as Λ baryons and K_S^0 mesons, and hadrons produced in material interactions, is obtained using tracks with a large estimated effective impact parameter with respect to the mean of the PV distribution. The abundance of electrons from γ conversions, which is considerable at low p_T , is validated using particle identification detectors.

Additionally, bin migration effects due to the resolution of the detector are found to have a negligible contribution to the measured yields. A minor correction is made since the mass of the particle is ignored in the expression

$\eta = \eta_{\text{lab}} - 0.465$ which is used to translate the pseudorapidity in the laboratory system to the center-of-mass system of the nucleon-nucleon collision in $p\text{-Pb}$ collisions.

Several sources of systematic uncertainty are considered. For candidates in the range $5 < p < 200$ GeV/ c the track-finding efficiency carries an uncertainty due to the limited size of the calibration samples and the difference between hadron and muon material interactions. For candidates outside this range, a conservative 5% uncertainty is assigned based on the efficiency variation in adjacent intervals. An uncertainty is assigned accounting for the detector occupancy description, which is estimated considering alternative weights. The uncertainty due to imperfect knowledge of the relative particle composition is determined from a 30% variation in the relative abundances of particles obtained from simulation. The uncertainty on the selection efficiency originates primarily from the limited size of the calibration sample. For the purity, the systematic uncertainty is estimated from the background abundance in the background-enriched samples and the data-simulation discrepancy in the background fraction from the independent samples. This uncertainty has a large η and p_T dependence: while negligible in regions with a small background level, it is the dominant contribution for intervals with large background contributions. These intervals correspond to high p_T for fake tracks in $p\text{-Pb}$ collisions in the backward region. See the Supplemental Material [48] for a summary table of the uncertainties.

The measured prompt charged particle cross sections for pp and $p\text{-Pb}$ are presented in Fig. 1. The total uncertainty is the sum in quadrature of statistical, systematic, and luminosity uncertainties. On average 0.1035 ± 0.0029 charged particles (with $0.961 < p_T < 1.249$ GeV/ c and $3.0 < \eta < 3.5$) are produced in pp collisions, when scaled by the total inelastic nucleon-nucleon cross section of 67.6 ± 0.6 mb at $\sqrt{s_{\text{NN}}} = 5$ TeV [49]. This is 2 orders of magnitude smaller than for $p\text{-Pb}$ collisions, assuming the

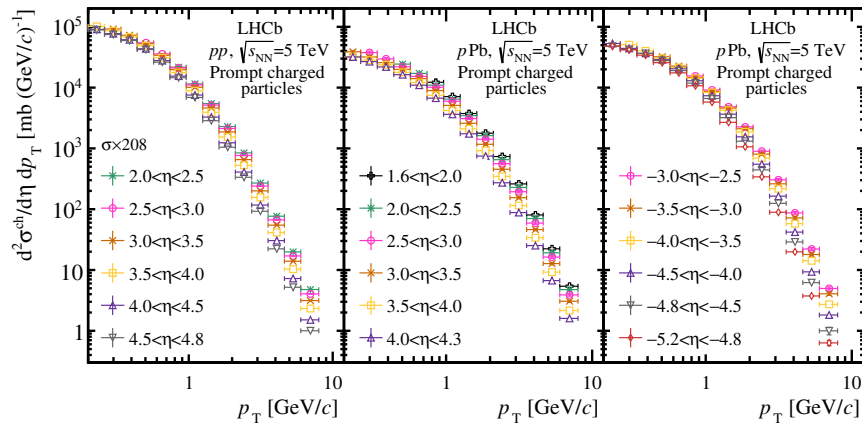


FIG. 1. Differential cross section of prompt charged particle production as a function of p_T in different η intervals in (left) pp , (middle) forward $p\text{-Pb}$, and (right) backward $p\text{-Pb}$ collisions. The cross section values for pp are scaled by the lead mass number ($A = 208$) for comparison with the $p\text{-Pb}$ cross sections.

same total inelastic nucleon-nucleon cross section. The cross section for $p\bar{p}$ collisions at $\sqrt{s_{NN}} = 5$ TeV is compared with the result at $\sqrt{s_{NN}} = 13$ TeV [27]. Both results are consistent, showing an increase in the cross section at 13 TeV of a factor 1 to 3, depending on p_T .

The result for $R_{p\text{Pb}}$ in different (η, p_T) intervals is presented in Fig. 2, where the uncertainties arise from statistical, systematic, and luminosity sources. In the forward region, the measurement indicates a suppression of charged particle production in $p\text{-Pb}$ collisions relative to that in $p\bar{p}$ collisions, which increases towards forward pseudorapidities. In the low p_T regime, $R_{p\text{Pb}}$ reaches values of about 0.3 in the most forward pseudorapidities. In the backward region, a significant enhancement of $R_{p\text{Pb}}$ is observed for $p_T > 1.5$ GeV/c. This can be interpreted as Cronin enhancement [15]. The enhancement reaches a maximum at different p_T values depending on η , followed by a decreasing trend towards unity. This decrease is more pronounced in the most backward pseudorapidities. The maximum value of $R_{p\text{Pb}}$ is found to be ~ 1.3 and depends slightly on η .

The $R_{p\text{Pb}}$ measurement is compared in Fig. 2 with predictions from phenomenological models covering the $p_T \gtrsim 1.5$ GeV/c region. The prediction in Ref. [50] (shaded green) is based on the NPDF set EPPS16 [10] for the lead nucleus and the PDF set CT14 [52] for the proton. The calculation also employs the parton-to-hadron fragmentation functions set DSS [53]. The prediction reproduces the data in the forward region although with large uncertainties. However, it fails to reproduce the $R_{p\text{Pb}}$ enhancement in the backward region for $p_T > 2$ GeV/c.

The second prediction (violet) is based on the CGC effective field theory [20]. The model is only applicable to

the saturation region at low x and thus to forward rapidities. The predicted gradual decrease of $R_{p\text{Pb}}$ with η is observed in the data, although the prediction overestimates $R_{p\text{Pb}}$ in the lower p_T intervals. The prediction does not include an uncertainty estimation.

The third prediction (shaded orange) is a PQCD calculation within the high-twist factorization formalism in the backward region [13,51]. The calculation shows an enhancement due to incoherent multiple scattering inside the nucleus before and after the hard scattering, and reproduces the enhancement seen in $p\text{-Au}$ collisions in the backward region by the PHENIX experiment at $\sqrt{s_{NN}} = 200$ GeV [25]. The prediction shows a p_T trend similar to data for $p_T > 3$ GeV/c in the most backward η interval, although it does not reproduce the data for the other intervals in the backward configuration.

Understanding the evolution of $R_{p\text{Pb}}$ with x and the momentum transfer Q^2 , is a critical point for the study of CNM effects. However, x and Q^2 are partonic quantities and cannot be directly measured. Instead, experimental proxies for x and Q^2 [54], defined as

$$Q_{\text{exp}}^2 \equiv m^2 + p_T^2 \quad \text{and} \quad x_{\text{exp}} \equiv \frac{Q_{\text{exp}}}{\sqrt{s_{NN}}} e^{-\eta}, \quad (3)$$

are considered to compare the $R_{p\text{Pb}}$ results among different LHC experiments. Here, m is the mass of the produced particle and is taken as $m = 256$ MeV/c², the average charged particle mass in $p\text{-Pb}$ collisions determined with EPOS-LHC. The variable x_{exp} is approximately x for a two body scattering, and Q_{exp} is the transverse mass of the produced particle.

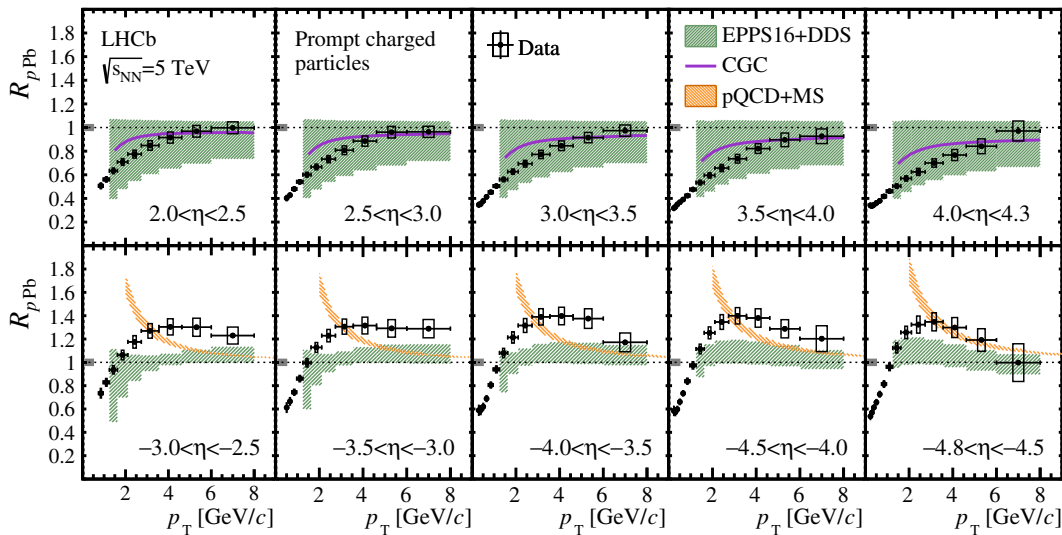


FIG. 2. Nuclear modification factor as a function of p_T in different η intervals for the (top) forward and (bottom) backward regions, compared with the predictions from Refs. [13,20,50,51]. Vertical error bars correspond to statistical uncertainties, open boxes to uncorrelated systematic uncertainty, and the filled box at $R_{p\text{Pb}} = 1$ to the correlated uncertainty from the luminosity.

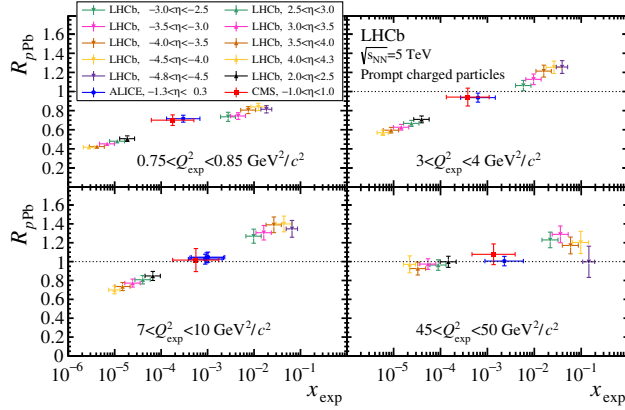


FIG. 3. Evolution of the nuclear modification factor with x_{exp} from this study, ALICE [21], and CMS [22], for different Q_{exp}^2 ranges. Each plot includes all the $R_{p\text{Pb}}$ (η, p_T) intervals with a p_T center within the Q_{exp}^2 range specified in the plot. Horizontal error bars account for the minimum and maximum x_{exp} value for a given (η, p_T) interval. Vertical error bars correspond to statistical, systematic, and luminosity (normalization) uncertainties for LHCb (ALICE, CMS), added in quadrature.

Figure 3 shows the $R_{p\text{Pb}}$ evolution with x_{exp} for four Q_{exp}^2 intervals from this study and the results from the ALICE [21] and CMS [22] Collaborations. Since the p_T binning is different among the three experiments, the Q_{exp}^2 ranges are selected to contain at least one p_T interval from each experiment. A consistent trend between this measurement in the forward region, the measurements in the central region from ALICE and CMS, and the result in the backward region, is observed for the four Q_{exp}^2 intervals. The evolution of $R_{p\text{Pb}}$ with x_{exp} is Q_{exp}^2 dependent.

In summary, the differential production cross sections have been measured in p_T and η intervals for prompt charged particles produced in pp and $p\text{-Pb}$ collisions at $\sqrt{s_{\text{NN}}} = 5 \text{ TeV}$. The measurement corresponds to $p > 2 \text{ GeV}/c$ and $0.2 < p_T < 8.0 \text{ GeV}/c$ prompt charged particles with $2.0 < \eta < 4.8$ in pp and $-5.2 < \eta < -2.5$ and $1.5 < \eta < 4.3$ in $p\text{-Pb}$ collisions. This is the first determination of such cross sections in $p\text{-Pb}$ collisions in the forward and backward regions at the LHC, and the first measurement in pp collisions at $\sqrt{s_{\text{NN}}} = 5 \text{ TeV}$. The total uncertainty is around 3% for most kinematic intervals both in pp and $p\text{-Pb}$ collisions. As a result, the data place stringent constraints on nonperturbative QCD models in high-energy nuclear collisions.

The nuclear modification factor $R_{p\text{Pb}}$ is also determined and is one of the most precise to date. The total uncertainty, including the normalization contribution, is below 5% for most of the (η, p_T) intervals. In the forward region, a suppression of the charged particle production is observed, especially for low p_T and the most forward η . In the backward region, the production of charged particles with $p_T > 1.5 \text{ GeV}/c$ is significantly enhanced. The $R_{p\text{Pb}}$ shape

exhibits a clear pseudorapidity dependence. These data cannot be simultaneously described across the entire measured η range by NPDFs alone. Contrary to what is observed at central rapidity [18], the forward data are inconsistent with CGC calculations at the lowest p_T . Multiple scattering calculations, which successfully reproduce PHENIX results [25], fail to describe the backward region. These measurements provide strong constraints on nuclear PDFs at the lowest accessible x ranges, and show that additional, previously unconsidered mechanisms are required to provide a consistent description of particle production in nuclear collisions at the LHC.

We would like to thank to Hannu Paukkunen, Ilka Helenius, Heikki Mäntysaari, and Zhong-Bo Kang, for providing LHCb specific theoretical predictions. We express our gratitude to our colleagues in the CERN accelerator departments for the excellent performance of the LHC. We thank the technical and administrative staff at the LHCb institutes. We acknowledge support from CERN and from the national agencies: CAPES, CNPq, FAPERJ and FINEP (Brazil); MOST and NSFC (China); CNRS/IN2P3 (France); BMBF, DFG and MPG (Germany); INFN (Italy); NWO (Netherlands); MNiSW and NCN (Poland); MEN/IFA (Romania); MSHE (Russia); MICINN (Spain); SNSF and SER (Switzerland); NASU (Ukraine); STFC (United Kingdom); DOE NP and NSF (USA). We acknowledge the computing resources that are provided by CERN, IN2P3 (France), KIT, and DESY (Germany), INFN (Italy), SURF (Netherlands), PIC (Spain), GridPP (United Kingdom), RRCKI and Yandex LLC (Russia), CSCS (Switzerland), IFIN-HH (Romania), CBPF (Brazil), PL-GRID (Poland) and OSC (USA). We are indebted to the communities behind the multiple open-source software packages on which we depend. Individual groups or members have received support from AvH Foundation (Germany); EPLANET, Marie Skłodowska-Curie Actions and ERC (European Union); A*MIDEX, ANR, Labex P2IO and OCEVU, and Région Auvergne-Rhône-Alpes (France); Key Research Program of Frontier Sciences of CAS, CAS PIFI, Thousand Talents Program, and Sci. & Tech. Program of Guangzhou (China); RFBR, RSF and Yandex LLC (Russia); GVA, XuntaGal and GENCAT (Spain); the Royal Society and the Leverhulme Trust (United Kingdom).

-
- [1] A. B. Kaidalov and K. A. Ter-Martirosyan, Multihadron production at high energies in the model of quark gluon strings, Sov. J. Nucl. Phys. **40**, 135 (1984), <https://inspirehep.net/literature/198183>.
 - [2] A. Capella, U. Sukhatme, C.-I. Tan, and J. Tran Thanh Van, Dual parton model, Phys. Rep. **236**, 225 (1994).
 - [3] A. Buckley *et al.*, General-purpose event generators for LHC physics, Phys. Rep. **504**, 145 (2011).

- [4] D. d'Enterria, R. Engel, T. Pierog, S. Ostapchenko, and K. Werner, Constraints from the first LHC data on hadronic event generators for ultra-high energy cosmic-ray physics, *Astropart. Phys.* **35**, 98 (2011).
- [5] J. Albrecht *et al.*, The Muon Puzzle in cosmic-ray induced air showers and its connection to the Large Hadron Collider, [arXiv:2105.06148](#).
- [6] C. A. Salgado *et al.*, Proton-nucleus collisions at the LHC: Scientific opportunities and requirements, *J. Phys. G* **39**, 015010 (2012).
- [7] J. L. Albacete *et al.*, Predictions for $p + \text{Pb}$ collisions at $\sqrt{s_{NN}} = 5$ TeV, *Int. J. Mod. Phys. E* **22**, 1330007 (2013).
- [8] J. L. Albacete *et al.*, Predictions for cold nuclear matter effects in $p + \text{Pb}$ collisions at $\sqrt{s_{NN}} = 8.16$ TeV, *Nucl. Phys.* **A972**, 18 (2018).
- [9] J. L. Nagle and W. A. Zajc, Small system collectivity in relativistic hadronic and nuclear collisions, *Annu. Rev. Nucl. Part. Sci.* **68**, 211 (2018).
- [10] K. J. Eskola, P. Paakkinen, H. Paukkunen, and C. A. Salgado, EPPS16: Nuclear parton distributions with LHC data, *Eur. Phys. J. C* **77**, 163 (2017).
- [11] K. Kovářík, A. Kusina, T. Ježo, D. B. Clark, C. Keppel, F. Lyonnet, J. G. Morfín, F. I. Olness, J. F. Owens, I. Schienbein, and J. Y. Yu, nCTEQ15—Global analysis of nuclear parton distributions with uncertainties in the CTEQ framework, *Phys. Rev. D* **93**, 085037 (2016).
- [12] D. de Florian, R. Sassot, P. Zurita, and M. Stratmann, Global analysis of nuclear parton distributions, *Phys. Rev. D* **85**, 074028 (2012).
- [13] Z.-B. Kang, I. Vitev, and H. Xing, Multiple scattering effects on inclusive particle production in the large-x regime, *Phys. Rev. D* **88**, 054010 (2013).
- [14] A. Accardi, Cronin effect in proton nucleus collisions: A survey of theoretical models, [arXiv:hep-ph/0212148](#).
- [15] J. W. Cronin, H. J. Frisch, M. J. Shochet, J. P. Boymond, P. A. Piroué, and R. L. Sumner, Production of hadrons with large transverse momentum at 200, 300, and 400 GeV, *Phys. Rev. D* **11**, 3105 (1975).
- [16] H. Kowalski, T. Lappi, and R. Venugopalan, Nuclear Enhancement of Universal Dynamics of High Parton Densities, *Phys. Rev. Lett.* **100**, 022303 (2008).
- [17] L. D. McLerran and R. Venugopalan, Gluon distribution functions for very large nuclei at small transverse momentum, *Phys. Rev. D* **49**, 3352 (1994).
- [18] S. Acharya *et al.* (ALICE Collaboration), Nuclear modification factor of light neutral-meson spectra up to high transverse momentum in p-Pb collisions at $\sqrt{s_{NN}} = 8.16$ TeV, *Phys. Lett. B* **827**, 136943 (2022).
- [19] F. Arleo, F. Cougoulic, and S. Peigné, Fully coherent energy loss effects on light hadron production in pA collisions, *J. High Energy Phys.* **09** (2020) 190.
- [20] T. Lappi and H. Mäntysaari, Single inclusive particle production at high energy from HERA data to proton-nucleus collisions, *Phys. Rev. D* **88**, 114020 (2013).
- [21] S. Acharya *et al.* (ALICE Collaboration), Transverse momentum spectra and nuclear modification factors of charged particles in pp, p-Pb and Pb-Pb collisions at the LHC, *J. High Energy Phys.* **11** (2018) 013.
- [22] V. Khachatryan *et al.* (CMS Collaboration), Charged-particle nuclear modification factors in PbPb and pPb collisions at $\sqrt{s_{NN}} = 5.02$ TeV, *J. High Energy Phys.* **04** (2017) 039.
- [23] G. Aad *et al.* (ATLAS Collaboration), Transverse momentum, rapidity, and centrality dependence of inclusive charged-particle production in $\sqrt{s_{NN}} = 5.02$ TeV $p + \text{Pb}$ collisions measured by the ATLAS experiment, *Phys. Lett. B* **763**, 313 (2016).
- [24] I. Arsene *et al.* (BRAHMS Collaboration), On the Evolution of the Nuclear Modification Factors with Rapidity and Centrality in $d + \text{Au}$ Collisions at $\sqrt{s_{NN}} = 200$ GeV, *Phys. Rev. Lett.* **93**, 242303 (2004).
- [25] C. Aidala *et al.* (PHENIX Collaboration), Nuclear-modification factor of charged hadrons at forward and backward rapidity in $p + \text{Al}$ and $p + \text{Au}$ collisions at $\sqrt{s_{NN}} = 200$ GeV, *Phys. Rev. C* **101**, 034910 (2020).
- [26] B. B. Back *et al.* (PHOBOS Collaboration), Pseudorapidity dependence of charged hadron transverse momentum spectra in $d + \text{Au}$ collisions at $\sqrt{s_{NN}} = 200$ GeV, *Phys. Rev. C* **70**, 061901 (2004).
- [27] R. Aaij *et al.* (LHCb Collaboration), Measurement of prompt charged-particle production in proton-proton collisions at $\sqrt{s} = 13$ TeV, *J. High Energy Phys.* **01** (2022) 166.
- [28] S. Acharya *et al.* (ALICE Collaboration), The ALICE definition of primary particles, Report No. ALICE-PUBLIC-2017-005, CERN, 2017.
- [29] A. A. Alves Jr. *et al.* (LHCb Collaboration), The LHCb detector at the LHC, *J. Instrum.* **3**, S08005 (2008).
- [30] R. Aaij *et al.* (LHCb Collaboration), LHCb detector performance, *Int. J. Mod. Phys. A* **30**, 1530022 (2015).
- [31] R. Aaij *et al.* (LHCb Collaboration), Precision luminosity measurements at LHCb, *J. Instrum.* **9**, P12005 (2014).
- [32] T. Pierog, I. Karpenko, J. M. Katzy, E. Yatsenko, and K. Werner, EPOS LHC: Test of collective hadronization with data measured at the CERN Large Hadron Collider, *Phys. Rev. C* **92**, 034906 (2015).
- [33] T. Sjöstrand, S. Mrenna, and P. Skands, A brief introduction to PYTHIA8.1, *Comput. Phys. Commun.* **178**, 852 (2008).
- [34] I. Belyaev *et al.*, Handling of the generation of primary events in Gauss, the LHCb simulation framework, *J. Phys. Conf. Ser.* **331**, 032047 (2011).
- [35] D. J. Lange, The EvtGen particle decay simulation package, *Nucl. Instrum. Methods Phys. Res., Sect. A* **462**, 152 (2001).
- [36] S. Agostinelli *et al.* (Geant4 Collaboration), GEANT4: A simulation toolkit, *Nucl. Instrum. Methods Phys. Res., Sect. A* **506**, 250 (2003).
- [37] J. Allison *et al.* (Geant4 Collaboration), Geant4 developments and applications, *IEEE Trans. Nucl. Sci.* **53**, 270 (2006).
- [38] M. Clemencic, G. Corti, S. Easo, C. R. Jones, S. Miglioranza, M. Pappagallo, and P. Robbe, The LHCb simulation application, Gauss: Design, evolution and experience, *J. Phys. Conf. Ser.* **331**, 032023 (2011).
- [39] M. De Cian, S. Farry, P. Seyfert, and S. Stahl, Fast neural-net based fake track rejection in the LHCb reconstruction, Report No. LHCb-PUB-2017-011, 2017.
- [40] R. Aaij *et al.* (LHCb Collaboration), Measurement of the track reconstruction efficiency at LHCb, *J. Instrum.* **10**, P02007 (2015).
- [41] J. Adam *et al.* (ALICE Collaboration), Multiplicity dependence of charged pion, kaon, and (anti)proton production

- at large transverse momentum in p-Pb collisions at $\sqrt{s_{NN}} = 5.02$ TeV, *Phys. Lett. B* **760**, 720 (2016).
- [42] J. Adam *et al.* (ALICE Collaboration), Enhanced production of multi-strange hadrons in high-multiplicity proton-proton collisions, *Nat. Phys.* **13**, 535 (2017).
- [43] J. Adam *et al.* (ALICE Collaboration), Multi-strange baryon production in p-Pb collisions at $\sqrt{s_{NN}} = 5.02$ TeV, *Phys. Lett. B* **758**, 389 (2016).
- [44] B. B. Abelev *et al.* (ALICE Collaboration), Multiplicity dependence of pion, kaon, proton and lambda production in p-Pb collisions at $\sqrt{s_{NN}} = 5.02$ TeV, *Phys. Lett. B* **728**, 25 (2014).
- [45] R. Aaij *et al.* (LHCb Collaboration), Measurement of prompt hadron production ratios in $p + p$ collisions at $\sqrt{s} = 0.9$ and 7 TeV, *Eur. Phys. J. C* **72**, 2168 (2012).
- [46] T. Sjöstrand, S. Ask, J. R. Christiansen, R. Corke, N. Desai, P. Ilten, S. Mrenna, S. Prestel, C. O. Rasmussen, and P. Z. Skands, An introduction to PYTHIA8.2, *Comput. Phys. Commun.* **191**, 159 (2015).
- [47] C. Bierlich, Microscopic collectivity: The ridge and strangeness enhancement from string-string interactions, *Nucl. Phys.* **A982**, 499 (2019).
- [48] See Supplemental Material at <http://link.aps.org/supplemental/10.1103/PhysRevLett.128.142004> for a summary table of the uncertainties.
- [49] C. Loizides, J. Kamin, and D. d'Enterria, Improved Monte Carlo Glauber predictions at present and future nuclear colliders, *Phys. Rev. C* **97**, 054910 (2018); **99**, 019901(E) (2019).
- [50] I. Helenius, K. J. Eskola, and H. Paukkunen, Probing the small- x nuclear gluon distributions with isolated photons at forward rapidities in $p + Pb$ collisions at the LHC, *J. High Energy Phys.* **09** (2014) 138.
- [51] Z.-B. Kang, I. Vitev, E. Wang, H. Xing, and C. Zhang, Multiple scattering effects on heavy meson production in $p + A$ collisions at backward rapidity, *Phys. Lett. B* **740**, 23 (2015).
- [52] S. Dulat, T.-J. Hou, J. Gao, M. Guzzi, J. Huston, P. Nadolsky, J. Pumplin, C. Schmidt, D. Stump, and C.-P. Yuan, New parton distribution functions from a global analysis of quantum chromodynamics, *Phys. Rev. D* **93**, 033006 (2016).
- [53] D. de Florian, R. Sassot, and M. Stratmann, Global analysis of fragmentation functions for pions and kaons and their uncertainties, *Phys. Rev. D* **75**, 114010 (2007).
- [54] N. Armesto, Nuclear shadowing, *J. Phys. G* **32**, R367 (2006).

R. Aaij,³² C. Abellán Beteta,⁵⁰ T. Ackernley,⁶⁰ B. Adeva,⁴⁶ M. Adinolfi,⁵⁴ H. Afsharnia,⁹ C. A. Aidala,⁸⁶ S. Aiola,²⁵ Z. Ajaltouni,⁹ S. Akar,⁶⁵ J. Albrecht,¹⁵ F. Alessio,⁴⁸ M. Alexander,⁵⁹ A. Alfonso Albero,⁴⁵ Z. Aliouche,⁶² G. Alkhazov,³⁸ P. Alvarez Cartelle,⁵⁵ S. Amato,² J. L. Amey,⁵⁴ Y. Amhis,¹¹ L. An,⁴⁸ L. Anderlini,²² A. Andreianov,³⁸ M. Andreotti,²¹ F. Archilli,¹⁷ A. Artamonov,⁴⁴ M. Artuso,⁶⁸ K. Arzymatov,⁴² E. Aslanides,¹⁰ M. Atzeni,⁵⁰ B. Audurier,¹² S. Bachmann,¹⁷ M. Bachmayer,⁴⁹ J. J. Back,⁵⁶ P. Baladron Rodriguez,⁴⁶ V. Balagura,¹² W. Baldini,²¹ J. Baptista Leite,¹ R. J. Barlow,⁶² S. Barsuk,¹¹ W. Barter,⁶¹ M. Bartolini,^{24,a} F. Baryshnikov,⁸³ J. M. Basels,¹⁴ G. Bassi,²⁹ B. Batsukh,⁶⁸ A. Battig,¹⁵ A. Bay,⁴⁹ M. Becker,¹⁵ F. Bedeschi,²⁹ I. Bediaga,¹ A. Beiter,⁶⁸ V. Belavin,⁴² S. Belin,²⁷ V. Bellee,⁴⁹ K. Belous,⁴⁴ I. Belov,⁴⁰ I. Belyaev,⁴¹ G. Bencivenni,²³ E. Ben-Haim,¹³ A. Berezhnoy,⁴⁰ R. Bernet,⁵⁰ D. Berninghoff,¹⁷ H. C. Bernstein,⁶⁸ C. Bertella,⁴⁸ A. Bertolin,²⁸ C. Betancourt,⁵⁰ F. Betti,⁴⁸ Ia. Bezshyiko,⁵⁰ S. Bhasin,⁵⁴ J. Bhom,³⁵ L. Bian,⁷³ M. S. Bieker,¹⁵ S. Bifani,⁵³ P. Billoir,¹³ M. Birch,⁶¹ F. C. R. Bishop,⁵⁵ A. Bitadze,⁶² A. Bizzeti,^{22,b} M. Bjørn,⁶³ M. P. Blago,⁴⁸ T. Blake,⁵⁶ F. Blanc,⁴⁹ S. Blusk,⁶⁸ D. Bobulska,⁵⁹ J. A. Boelhauve,¹⁵ O. Boente Garcia,⁴⁶ T. Boettcher,⁶⁵ A. Boldyrev,⁸² A. Bondar,⁴³ N. Bondar,^{38,48} S. Borghi,⁶² M. Borisjak,⁴² M. Borsato,¹⁷ J. T. Borsuk,³⁵ S. A. Bouchiba,⁴⁹ T. J. V. Bowcock,⁶⁰ A. Boyer,⁴⁸ C. Bozzi,²¹ M. J. Bradley,⁶¹ S. Braun,⁶⁶ A. Brea Rodriguez,⁴⁶ M. Brodski,⁴⁸ J. Brodzicka,³⁵ A. Brossa Gonzalo,⁵⁶ D. Brundu,²⁷ A. Buonaura,⁵⁰ A. T. Burke,⁶² C. Burr,⁴⁸ A. Bursche,⁷² A. Butkevich,³⁹ J. S. Butter,³² J. Buytaert,⁴⁸ W. Byczynski,⁴⁸ S. Cadeddu,²⁷ H. Cai,⁷³ R. Calabrese,^{21,c} L. Calefice,^{15,13} L. Calero Diaz,²³ S. Cali,²³ R. Calladine,⁵³ M. Calvi,^{26,d} M. Calvo Gomez,⁸⁵ P. Camargo Magalhaes,⁵⁴ P. Campana,²³ A. F. Campoverde Quezada,⁶ S. Capelli,^{26,d} L. Capriotti,^{20,e} A. Carbone,^{20,e} G. Carboni,³¹ R. Cardinale,^{24,a} A. Cardini,²⁷ I. Carli,⁴ P. Carniti,^{26,d} L. Carus,¹⁴ K. Carvalho Akiba,³² A. Casais Vidal,⁴⁶ G. Casse,⁶⁰ M. Cattaneo,⁴⁸ G. Cavallero,⁴⁸ S. Celani,⁴⁹ J. Cerasoli,¹⁰ A. J. Chadwick,⁶⁰ M. G. Chapman,⁵⁴ M. Charles,¹³ Ph. Charpentier,⁴⁸ G. Chatzikonstantinidis,⁵³ C. A. Chavez Barajas,⁶⁰ M. Chefdeville,⁸ C. Chen,³ S. Chen,⁴ A. Chernov,³⁵ V. Chobanova,⁴⁶ S. Cholak,⁴⁹ M. Chrzaszcz,³⁵ A. Chubykin,³⁸ V. Chulikov,³⁸ P. Ciambrone,²³ M. F. Cicala,⁵⁶ X. Cid Vidal,⁴⁶ G. Ciezarek,⁴⁸ P. E. L. Clarke,⁵⁸ M. Clemencic,⁴⁸ H. V. Cliff,⁵⁵ J. Closier,⁴⁸ J. L. Cobbley,⁶² V. Coco,⁴⁸ J. A. B. Coelho,¹¹ J. Cogan,¹⁰ E. Cogneras,⁹ L. Cojocariu,³⁷ P. Collins,⁴⁸ T. Colombo,⁴⁸ L. Congedo,^{19,f} A. Contu,²⁷ N. Cooke,⁵³ G. Coombs,⁵⁹ I. Corredoira,⁴⁶ G. Corti,⁴⁸ C. M. Costa Sobral,⁵⁶ B. Couturier,⁴⁸ D. C. Craik,⁶⁴ J. Crkovská,⁶⁷ M. Cruz Torres,¹ R. Currie,⁵⁸ C. L. Da Silva,⁶⁷ S. Dadabaev,⁸³ L. Dai,⁷¹ E. Dall'Occo,¹⁵ J. Dalseno,⁴⁶ C. D'Ambrosio,⁴⁸ A. Danilina,⁴¹ P. d'Argent,⁴⁸ J. E. Davies,⁶² A. Davis,⁶² O. De Aguiar Francisco,⁶² K. De Bruyn,⁷⁹ S. De Capua,⁶² M. De Cian,⁴⁹ J. M. De Miranda,¹ L. De Paula,² M. De Serio,^{19,f} D. De Simone,⁵⁰ P. De Simone,²³ J. A. de Vries,⁸⁰ C. T. Dean,⁶⁷ D. Decamp,⁸ L. Del Buono,¹³ B. Delaney,⁵⁵

- H.-P. Dembinski,¹⁵ A. Dendek,³⁴ V. Denysenko,⁵⁰ D. Derkach,⁸² O. Deschamps,⁹ F. Desse,¹¹ F. Dettori,^{27,g} B. Dey,⁷⁷
 A. Di Cicco,²³ P. Di Nezza,²³ S. Didenko,⁸³ L. Dieste Maronas,⁴⁶ H. Dijkstra,⁴⁸ V. Dobishuk,⁵² A. M. Donohoe,¹⁸
 F. Dordei,²⁷ A. C. dos Reis,¹ L. Douglas,⁵⁹ A. Dovbnya,⁵¹ A. G. Downes,⁸ K. Dreimanis,⁶⁰ M. W. Dudek,³⁵ L. Dufour,⁴⁸
 V. Duk,⁷⁸ P. Durante,⁴⁸ J. M. Durham,⁶⁷ D. Dutta,⁶² A. Dziurda,³⁵ A. Dzyuba,³⁸ S. Easo,⁵⁷ U. Egede,⁶⁹ V. Egorychev,⁴¹
 S. Eidelman,^{43,h} S. Eisenhardt,⁵⁸ S. Ek-In,⁴⁹ L. Eklund,^{59,i} S. Ely,⁶⁸ A. Ene,³⁷ E. Epple,⁶⁷ S. Escher,¹⁴ J. Eschle,⁵⁰ S. Esen,¹³
 T. Evans,⁴⁸ A. Falabella,²⁰ J. Fan,³ Y. Fan,⁶ B. Fang,⁷³ S. Farry,⁶⁰ D. Fazzini,^{26,d} M. Féo,⁴⁸ A. Fernandez Prieto,⁴⁶
 A. D. Fernez,⁶⁶ F. Ferrari,^{20,e} L. Ferreira Lopes,⁴⁹ F. Ferreira Rodrigues,² S. Ferreres Sole,³² M. Ferrillo,⁵⁰ M. Ferro-Luzzi,⁴⁸
 S. Filippov,³⁹ R. A. Fini,¹⁹ M. Fiorini,^{21,c} M. Firlej,³⁴ K. M. Fischer,⁶³ D. S. Fitzgerald,⁸⁶ C. Fitzpatrick,⁶² T. Fiutowski,³⁴
 A. Fkiaras,⁴⁸ F. Fleuret,¹² M. Fontana,¹³ F. Fontanelli,^{24,a} R. Forty,⁴⁸ V. Franco Lima,⁶⁰ M. Franco Sevilla,⁶⁶ M. Frank,⁴⁸
 E. Franzoso,²¹ G. Frau,¹⁷ C. Frei,⁴⁸ D. A. Friday,⁵⁹ J. Fu,²⁵ Q. Fuehring,¹⁵ W. Funk,⁴⁸ E. Gabriel,³² T. Gaintseva,⁴²
 A. Gallas Torreira,⁴⁶ D. Galli,^{20,e} S. Gambetta,^{58,48} Y. Gan,³ M. Gandelman,² P. Gandini,²⁵ Y. Gao,⁵ M. Garau,²⁷
 L. M. Garcia Martin,⁵⁶ P. Garcia Moreno,⁴⁵ J. García Pardiñas,^{26,d} B. Garcia Plana,⁴⁶ F. A. Garcia Rosales,¹² L. Garrido,⁴⁵
 C. Gaspar,⁴⁸ R. E. Geertsema,³² D. Gerick,¹⁷ L. L. Gerken,¹⁵ E. Gersabeck,⁶² M. Gersabeck,⁶² T. Gershon,⁵⁶ D. Gerstel,¹⁰
 Ph. Ghez,⁸ V. Gibson,⁵⁵ H. K. Giemza,³⁶ M. Giovannetti,^{23,j} A. Gioventù,⁴⁶ P. Gironella Gironell,⁴⁵ L. Giubega,³⁷
 C. Giugliano,^{21,48,c} K. Gizzov,⁵⁸ E. L. Gkougkousis,⁴⁸ V. V. Gligorov,¹³ C. Göbel,⁷⁰ E. Golobardes,⁸⁵ D. Golubkov,⁴¹
 A. Golutvin,^{61,83} A. Gomes,^{1,k} S. Gomez Fernandez,⁴⁵ F. Goncalves Abrantes,⁶³ M. Goncerz,³⁵ G. Gong,³ P. Gorbounov,⁴¹
 I. V. Gorelov,⁴⁰ C. Gotti,²⁶ E. Govorkova,⁴⁸ J. P. Grabowski,¹⁷ T. Grammatico,¹³ L. A. Granado Cardoso,⁴⁸ E. Graugés,⁴⁵
 E. Graverini,⁴⁹ G. Graziani,²² A. Grecu,³⁷ L. M. Greeven,³² P. Griffith,^{21,c} L. Grillo,⁶² S. Gromov,⁸³ B. R. Gruberg Cazon,⁶³
 C. Gu,³ M. Guarise,²¹ P. A. Günther,¹⁷ E. Gushchin,³⁹ A. Guth,¹⁴ Y. Guz,⁴⁴ T. Gys,⁴⁸ T. Hadavizadeh,⁶⁹ G. Haefeli,⁴⁹
 C. Haen,⁴⁸ J. Haimberger,⁴⁸ T. Halewood-leagas,⁶⁰ P. M. Hamilton,⁶⁶ J. P. Hammerich,⁶⁰ Q. Han,⁷ X. Han,¹⁷
 T. H. Hancock,⁶³ S. Hansmann-Menzemer,¹⁷ N. Harnew,⁶³ T. Harrison,⁶⁰ C. Hasse,⁴⁸ M. Hatch,⁴⁸ J. He,^{6,l} M. Hecker,⁶¹
 K. Heijhoff,³² K. Heinicke,¹⁵ A. M. Hennequin,⁴⁸ K. Hennessy,⁶⁰ L. Henry,⁴⁸ J. Heuel,¹⁴ A. Hicheur,² D. Hill,⁴⁹ M. Hilton,⁶²
 S. E. Hollitt,¹⁵ J. Hu,¹⁷ J. Hu,⁷² W. Hu,⁷ X. Hu,³ W. Huang,⁶ X. Huang,⁷³ W. Hulsbergen,³² R. J. Hunter,⁵⁶ M. Hushchyn,⁸²
 D. Hutchcroft,⁶⁰ D. Hynds,³² P. Ibis,¹⁵ M. Idzik,³⁴ D. Ilin,³⁸ P. Ilten,⁶⁵ A. Inglessi,³⁸ A. Ishteev,⁸³ K. Ivshin,³⁸ R. Jacobsson,⁴⁸
 S. Jakobsen,⁴⁸ E. Jans,³² B. K. Jashal,⁴⁷ A. Jawahery,⁶⁶ V. Jevtic,¹⁵ F. Jiang,³ M. John,⁶³ D. Johnson,⁴⁸ C. R. Jones,⁵⁵
 T. P. Jones,⁵⁶ B. Jost,⁴⁸ N. Jurik,⁴⁸ S. Kandybei,⁵¹ Y. Kang,³ M. Karacson,⁴⁸ M. Karpov,⁸² F. Keizer,⁴⁸ M. Kenzie,⁵⁶
 T. Ketel,³³ B. Khanji,¹⁵ A. Kharisova,⁸⁴ S. Kholodenko,⁴⁴ T. Kirn,¹⁴ V. S. Kirsebom,⁴⁹ O. Kitouni,⁶⁴ S. Klaver,³²
 K. Klimaszewski,³⁶ S. Koliev,⁵² A. Kondybayeva,⁸³ A. Konoplyannikov,⁴¹ P. Kopciewicz,³⁴ R. Kopecna,¹⁷
 P. Koppenburg,³² M. Korolev,⁴⁰ I. Kostiuk,^{32,52} O. Kot,⁵² S. Kotriakhova,^{21,38} P. Kravchenko,³⁸ L. Kravchuk,³⁹
 R. D. Krawczyk,⁴⁸ M. Kreps,⁵⁶ F. Kress,⁶¹ S. Kretzschmar,¹⁴ P. Krokovny,^{43,h} W. Krupa,³⁴ W. Krzemien,³⁶ W. Kucewicz,^{35,m}
 M. Kucharczyk,³⁵ V. Kudryavtsev,^{43,h} H. S. Kuindersma,^{32,33} G. J. Kunde,⁶⁷ T. Kvaratskheliya,⁴¹ D. Lacarrere,⁴⁸
 G. Lafferty,⁶² A. Lai,²⁷ A. Lampis,²⁷ D. Lancierini,⁵⁰ J. J. Lane,⁶² R. Lane,⁵⁴ G. Lanfranchi,²³ C. Langenbruch,¹⁴ J. Langer,¹⁵
 O. Lantwin,⁵⁰ T. Latham,⁵⁶ F. Lazzari,^{29,n} R. Le Gac,¹⁰ S. H. Lee,⁸⁶ R. Lefèvre,⁹ A. Leflat,⁴⁰ S. Legotin,⁸³ O. Leroy,¹⁰
 T. Lesiak,³⁵ B. Leverington,¹⁷ H. Li,⁷² L. Li,⁶³ P. Li,¹⁷ S. Li,⁷ Y. Li,⁴ Y. Li,⁴ Z. Li,⁶⁸ X. Liang,⁶⁸ T. Lin,⁶¹ R. Lindner,⁴⁸
 V. Lisovskyi,¹⁵ R. Litvinov,²⁷ G. Liu,⁷² H. Liu,⁶ S. Liu,⁴ A. Loi,²⁷ J. Lomba Castro,⁴⁶ I. Longstaff,⁵⁹ J. H. Lopes,²
 S. Lopez Solino,⁴⁶ G. H. Lovell,⁵⁵ Y. Lu,⁴ D. Lucchesi,^{28,o} S. Luchuk,³⁹ M. Lucio Martinez,³² V. Lukashenko,^{32,52} Y. Luo,³
 A. Lupato,⁶² E. Luppi,^{21,c} O. Lupton,⁵⁶ A. Lusiani,^{29,p} X. Lyu,⁶ L. Ma,⁴ R. Ma,⁶ S. Maccolini,^{20,e} F. Machefert,¹¹
 F. Maciuc,³⁷ V. Macko,⁴⁹ P. Mackowiak,¹⁵ S. Maddrell-Mander,⁵⁴ O. Madejczyk,³⁴ L. R. Madhan Mohan,⁵⁴ O. Maev,³⁸
 A. Maevskiy,⁸² D. Maisuzenko,³⁸ M. W. Majewski,³⁴ J. J. Malczewski,³⁵ S. Malde,⁶³ B. Malecki,⁴⁸ A. Malinin,⁸¹
 T. Maltsev,^{43,h} H. Malygina,¹⁷ G. Manca,^{27,g} G. Mancinelli,¹⁰ D. Manuzzi,^{20,e} D. Marangotto,^{25,q} J. Maratas,^{9,r}
 J. F. Marchand,⁸ U. Marconi,²⁰ S. Mariami,^{22,s} C. Marin Benito,⁴⁸ M. Marinangeli,⁴⁹ J. Marks,¹⁷ A. M. Marshall,⁵⁴
 P. J. Marshall,⁶⁰ G. Martellotti,³⁰ L. Martinazzoli,^{48,d} M. Martinelli,^{26,d} D. Martinez Santos,⁴⁶ F. Martinez Vidal,⁴⁷
 A. Massafferri,¹ M. Materok,¹⁴ R. Matev,⁴⁸ A. Mathad,⁵⁰ Z. Mathe,⁴⁸ V. Matiunin,⁴¹ C. Matteuzzi,²⁶ K. R. Mattioli,⁸⁶
 A. Mauri,³² E. Maurice,¹² J. Mauricio,⁴⁵ M. Mazurek,⁴⁸ M. McCann,⁶¹ L. McConnell,¹⁸ T. H. McGrath,⁶² A. McNab,⁶²
 R. McNulty,¹⁸ J. V. Mead,⁶⁰ B. Meadows,⁶⁵ G. Meier,¹⁵ N. Meinert,⁷⁶ D. Melnychuk,³⁶ S. Meloni,^{26,d} M. Merk,^{32,80}
 A. Merli,²⁵ L. Meyer Garcia,² M. Mikhasenko,⁴⁸ D. A. Milanes,⁷⁴ E. Millard,⁵⁶ M. Milovanovic,⁴⁸ M.-N. Minard,⁸
 A. Minotti,²¹ L. Minzoni,^{21,c} S. E. Mitchell,⁵⁸ B. Mitreska,⁶² D. S. Mitzel,⁴⁸ A. Mödden,¹⁵ R. A. Mohammed,⁶³
 R. D. Moise,⁶¹ T. Mombächer,⁴⁶ I. A. Monroy,⁷⁴ S. Monteil,⁹ M. Morandin,²⁸ G. Morello,²³ M. J. Morello,^{29,p} J. Moron,³⁴
 A. B. Morris,⁷⁵ A. G. Morris,⁵⁶ R. Mountain,⁶⁸ H. Mu,³ F. Muheim,^{58,48} M. Mulder,⁴⁸ D. Müller,⁴⁸ K. Müller,⁵⁰

- C. H. Murphy,⁶³ D. Murray,⁶² P. Muzzetto,^{27,48} P. Naik,⁵⁴ T. Nakada,⁴⁹ R. Nandakumar,⁵⁷ T. Nanut,⁴⁹ I. Nasteva,² M. Needham,⁵⁸ I. Neri,²¹ N. Neri,^{25,9} S. Neubert,⁷⁵ N. Neufeld,⁴⁸ R. Newcombe,⁶¹ T. D. Nguyen,⁴⁹ C. Nguyen-Mau,^{49,t} E. M. Niel,¹¹ S. Nieswand,¹⁴ N. Nikitin,⁴⁰ N. S. Nolte,⁶⁴ C. Normand,⁸ C. Nunez,⁸⁶ A. Oblakowska-Mucha,³⁴ V. Obraztsov,⁴⁴ D. P. O'Hanlon,⁵⁴ R. Oldeman,^{27,g} M. E. Olivares,⁶⁸ C. J. G. Onderwater,⁷⁹ R. H. O'Neil,⁵⁸ A. Ossowska,³⁵ J. M. Otalora Goicochea,² T. Ovsiannikova,⁴¹ P. Owen,⁵⁰ A. Oyanguren,⁴⁷ B. Pagare,⁵⁶ P. R. Pais,⁴⁸ T. Pajero,⁶³ A. Palano,¹⁹ M. Palutan,²³ Y. Pan,⁶² G. Panshin,⁸⁴ A. Papanestis,⁵⁷ M. Pappagalio,^{19,f} L. L. Pappalardo,^{21,c} C. Pappenheimer,⁶⁵ W. Parker,⁶⁶ C. Parkes,⁶² C. J. Parkinson,⁴⁶ B. Passalacqua,²¹ G. Passaleva,²² A. Pastore,¹⁹ M. Patel,⁶¹ C. Patrignani,^{20,e} C. J. Pawley,⁸⁰ A. Pearce,⁴⁸ A. Pellegrino,³² M. Pepe Altarelli,⁴⁸ S. Perazzini,²⁰ D. Pereima,⁴¹ P. Perret,⁹ M. Petric,^{59,48} K. Petridis,⁵⁴ A. Petrolini,^{24,a} A. Petrov,⁸¹ S. Petrucci,⁵⁸ M. Petruzzo,²⁵ T. T. H. Pham,⁶⁸ A. Philippov,⁴² L. Pica,^{29,p} M. Piccini,⁷⁸ B. Pietrzyk,⁸ G. Pietrzyk,⁴⁹ M. Pili,⁶³ D. Pinci,³⁰ F. Pisani,⁴⁸ Resmi P. K,¹⁰ V. Placinta,³⁷ J. Plews,⁵³ M. Plo Casasus,⁴⁶ F. Polci,¹³ M. Poli Lener,²³ M. Poliakova,⁶⁸ A. Poluektov,¹⁰ N. Polukhina,^{83,u} I. Polyakov,⁶⁸ E. Polycarpo,² G. J. Pomery,⁵⁴ S. Ponce,⁴⁸ D. Popov,^{6,48} S. Popov,⁴² S. Poslavskii,⁴⁴ K. Prasant,³⁵ L. Promberger,⁴⁸ C. Prouve,⁴⁶ V. Pugatch,⁵² H. Pullen,⁶³ G. Punzi,^{29,v} H. Qi,³ W. Qian,⁶ J. Qin,⁶ N. Qin,³ R. Quagliani,¹³ B. Quintana,⁸ N. V. Raab,¹⁸ R. I. Rabadan Trejo,¹⁰ B. Rachwal,³⁴ J. H. Rademacker,⁵⁴ M. Rama,²⁹ M. Ramos Pernas,⁵⁶ M. S. Rangel,² F. Ratnikov,^{42,82} G. Raven,³³ M. Reboud,⁸ F. Redi,⁴⁹ F. Reiss,⁶² C. Remon Alepuz,⁴⁷ Z. Ren,³ V. Renaudin,⁶³ R. Ribatti,²⁹ S. Ricciardi,⁵⁷ K. Rinnert,⁶⁰ P. Robbe,¹¹ G. Robertson,⁵⁸ A. B. Rodrigues,⁴⁹ E. Rodrigues,⁶⁰ J. A. Rodriguez Lopez,⁷⁴ E. R. R. Rodriguez Rodriguez,⁴⁶ A. Rollings,⁶³ P. Roloff,⁴⁸ V. Romanovskiy,⁴⁴ M. Romero Lamas,⁴⁶ A. Romero Vidal,⁴⁶ J. D. Roth,⁸⁶ M. Rotondo,²³ M. S. Rudolph,⁶⁸ T. Ruf,⁴⁸ J. Ruiz Vidal,⁴⁷ A. Ryzhikov,⁸² J. Ryzka,³⁴ J. J. Saborido Silva,⁴⁶ N. Sagidova,³⁸ N. Sahoo,⁵⁶ B. Saitta,^{27,g} M. Salomoni,⁴⁸ C. Sanchez Gras,³² R. Santacesaria,³⁰ C. Santamarina Rios,⁴⁶ M. Santimaria,²³ E. Santovetti,^{31,j} D. Saranin,⁸³ G. Sarpis,¹⁴ M. Sarpis,⁷⁵ A. Sarti,³⁰ C. Satriano,^{30,w} A. Satta,³¹ M. Saur,¹⁵ D. Savrina,^{41,40} H. Sazak,⁹ L. G. Scantlebury Smead,⁶³ A. Scarabotto,¹³ S. Schael,¹⁴ M. Schiller,⁵⁹ H. Schindler,⁴⁸ M. Schmeling,¹⁶ B. Schmidt,⁴⁸ O. Schneider,⁴⁹ A. Schopper,⁴⁸ M. Schubiger,³² S. Schulte,⁴⁹ M. H. Schune,¹¹ R. Schwemmer,⁴⁸ B. Sciascia,²³ S. Sellam,⁴⁶ A. Semennikov,⁴¹ M. Senghi Soares,³³ A. Sergi,^{24,a} N. Serra,⁵⁰ L. Sestini,²⁸ A. Seuthe,¹⁵ P. Seyfert,⁴⁸ Y. Shang,⁵ D. M. Shangase,⁸⁶ M. Shapkin,⁴⁴ I. Shchemberov,⁸³ L. Shchutska,⁴⁹ T. Shears,⁶⁰ L. Shekhtman,^{43,h} Z. Shen,⁵ V. Shevchenko,⁸¹ E. B. Shields,^{26,d} E. Shmanin,⁸³ J. D. Shupperd,⁶⁸ B. G. Siddi,²¹ R. Silva Coutinho,⁵⁰ G. Simi,²⁸ S. Simone,^{19,f} N. Skidmore,⁶² T. Skwarnicki,⁶⁸ M. W. Slater,⁵³ I. Slazyk,^{21,c} J. C. Smallwood,⁶³ J. G. Smeaton,⁵⁵ A. Smetkina,⁴¹ E. Smith,⁵⁰ M. Smith,⁶¹ A. Snoch,³² M. Soares,²⁰ L. Soares Lavra,⁹ M. D. Sokoloff,⁶⁵ F. J. P. Soler,⁵⁹ A. Solovev,³⁸ I. Solovyev,³⁸ F. L. Souza De Almeida,² B. Souza De Paula,² B. Spaan,¹⁵ E. Spadaro Norella,^{25,q} P. Spradlin,⁵⁹ F. Stagni,⁴⁸ M. Stahl,⁶⁵ S. Stahl,⁴⁸ P. Stefkova,⁴⁹ O. Steinkamp,^{50,83} O. Stenyakin,⁴⁴ H. Stevens,¹⁵ S. Stone,⁶⁸ M. E. Stramaglia,⁴⁹ M. Stratificiuc,³⁷ D. Strekalina,⁸³ F. Suljik,⁶³ J. Sun,²⁷ L. Sun,⁷³ Y. Sun,⁶⁶ P. Svihra,⁶² P. N. Swallow,⁵³ K. Swientek,³⁴ A. Szabelski,³⁶ T. Szumlak,³⁴ M. Szymanski,⁴⁸ S. Taneja,⁶² A. R. Tanner,⁵⁴ A. Terentev,⁸³ F. Teubert,⁴⁸ E. Thomas,⁴⁸ D. J. D. Thompson,⁵³ K. A. Thomson,⁶⁰ V. Tisserand,⁹ S. T'Jampens,⁸ M. Tobin,⁴ L. Tomassetti,^{21,c} D. Torres Machado,¹ D. Y. Tou,¹³ M. T. Tran,⁴⁹ E. Trifonova,⁸³ C. Trippel,⁴⁹ G. Tuci,^{29,v} A. Tully,⁴⁹ N. Tuning,^{32,48} A. Ukleja,³⁶ D. J. Unverzagt,¹⁷ E. Ursov,⁸³ A. Usachov,³² A. Ustyuzhanin,^{42,82} U. Uwer,¹⁷ A. Vagner,⁸⁴ V. Vagnoni,²⁰ A. Valassi,⁴⁸ G. Valenti,²⁰ N. Valls Canudas,⁸⁵ M. van Beuzekom,³² M. Van Dijk,⁴⁹ E. van Herwijnen,⁸³ C. B. Van Hulse,¹⁸ M. van Veghel,⁷⁹ R. Vazquez Gomez,⁴⁵ P. Vazquez Regueiro,⁴⁶ C. Vázquez Sierra,⁴⁸ S. Vecchi,²¹ J. J. Velthuis,⁵⁴ M. Veltri,^{22,x} A. Venkateswaran,⁶⁸ M. Veronesi,³² M. Vesterinen,⁵⁶ D. Vieira,⁶⁵ M. Vieites Diaz,⁴⁹ H. Viemann,⁷⁶ X. Vilasis-Cardona,⁸⁵ E. Vilella Figueras,⁶⁰ A. Villa,²⁰ P. Vincent,¹³ D. Vom Bruch,¹⁰ A. Vorobyev,³⁸ V. Vorobyev,^{43,h} N. Voropaev,³⁸ K. Vos,⁸⁰ R. Waldi,¹⁷ J. Walsh,²⁹ C. Wang,¹⁷ J. Wang,⁵ J. Wang,⁴ J. Wang,³ J. Wang,⁷³ M. Wang,³ R. Wang,⁵⁴ Y. Wang,⁷ Z. Wang,⁵⁰ Z. Wang,³ H. M. Wark,⁶⁰ N. K. Watson,⁵³ S. G. Weber,¹³ D. Websdale,⁶¹ C. Weisser,⁶⁴ B. D. C. Westhenry,⁵⁴ D. J. White,⁶² M. Whitehead,⁵⁴ D. Wiedner,¹⁵ G. Wilkinson,⁶³ M. Wilkinson,⁶⁸ I. Williams,⁵⁵ M. Williams,⁶⁴ M. R. J. Williams,⁵⁸ F. F. Wilson,⁵⁷ W. Wislicki,³⁶ M. Witek,³⁵ L. Witola,¹⁷ G. Wormser,¹¹ S. A. Wotton,⁵⁵ H. Wu,⁶⁸ K. Wyllie,⁴⁸ Z. Xiang,⁶ D. Xiao,⁷ Y. Xie,⁷ A. Xu,⁵ J. Xu,⁶ L. Xu,³ M. Xu,⁷ Q. Xu,⁶ Z. Xu,⁵ Z. Xu,⁶ D. Yang,³ S. Yang,⁶ Y. Yang,⁶ Z. Yang,³ Z. Yang,⁶⁶ Y. Yao,⁶⁸ L. E. Yeomans,⁶⁰ H. Yin,⁷ J. Yu,⁷¹ X. Yuan,⁶⁸ O. Yushchenko,⁴⁴ E. Zaffaroni,⁴⁹ M. Zavertyaev,^{16,u} M. Zdybal,³⁵ O. Zenaiev,⁴⁸ M. Zeng,³ D. Zhang,⁷ L. Zhang,³ S. Zhang,⁷¹ S. Zhang,⁵ Y. Zhang,⁵ Y. Zhang,⁶³ A. Zharkova,⁸³ A. Zhelezov,¹⁷ Y. Zheng,⁶ X. Zhou,⁶ Y. Zhou,⁶ X. Zhu,³ Z. Zhu,⁶ V. Zhukov,^{14,40} J. B. Zonneveld,⁵⁸ Q. Zou,⁴ S. Zucchelli,^{20,e} D. Zuliani,²⁸ and G. Zunica⁶²

(LHCb Collaboration)

- ¹*Centro Brasileiro de Pesquisas Físicas (CBPF), Rio de Janeiro, Brazil*
- ²*Universidade Federal do Rio de Janeiro (UFRJ), Rio de Janeiro, Brazil*
- ³*Center for High Energy Physics, Tsinghua University, Beijing, China*
- ⁴*Institute Of High Energy Physics (IHEP), Beijing, China*
- ⁵*School of Physics State Key Laboratory of Nuclear Physics and Technology, Peking University, Beijing, China*
- ⁶*University of Chinese Academy of Sciences, Beijing, China*
- ⁷*Institute of Particle Physics, Central China Normal University, Wuhan, Hubei, China*
- ⁸*Univ. Savoie Mont Blanc, CNRS, IN2P3-LAPP, Annecy, France*
- ⁹*Université Clermont Auvergne, CNRS/IN2P3, LPC, Clermont-Ferrand, France*
- ¹⁰*Aix Marseille Univ, CNRS/IN2P3, CPPM, Marseille, France*
- ¹¹*Université Paris-Saclay, CNRS/IN2P3, IJCLab, Orsay, France*
- ¹²*Laboratoire Leprince-Ringuet, CNRS/IN2P3, Ecole Polytechnique, Institut Polytechnique de Paris, Palaiseau, France*
- ¹³*LPNHE, Sorbonne Université, Paris Diderot Sorbonne Paris Cité, CNRS/IN2P3, Paris, France*
- ¹⁴*I. Physikalisches Institut, RWTH Aachen University, Aachen, Germany*
- ¹⁵*Fakultät Physik, Technische Universität Dortmund, Dortmund, Germany*
- ¹⁶*Max-Planck-Institut für Kernphysik (MPIK), Heidelberg, Germany*
- ¹⁷*Physikalisches Institut, Ruprecht-Karls-Universität Heidelberg, Heidelberg, Germany*
- ¹⁸*School of Physics, University College Dublin, Dublin, Ireland*
- ¹⁹*INFN Sezione di Bari, Bari, Italy*
- ²⁰*INFN Sezione di Bologna, Bologna, Italy*
- ²¹*INFN Sezione di Ferrara, Ferrara, Italy*
- ²²*INFN Sezione di Firenze, Firenze, Italy*
- ²³*INFN Laboratori Nazionali di Frascati, Frascati, Italy*
- ²⁴*INFN Sezione di Genova, Genova, Italy*
- ²⁵*INFN Sezione di Milano, Milano, Italy*
- ²⁶*INFN Sezione di Milano-Bicocca, Milano, Italy*
- ²⁷*INFN Sezione di Cagliari, Monserrato, Italy*
- ²⁸*Università degli Studi di Padova, Università e INFN, Padova, Padova, Italy*
- ²⁹*INFN Sezione di Pisa, Pisa, Italy*
- ³⁰*INFN Sezione di Roma La Sapienza, Roma, Italy*
- ³¹*INFN Sezione di Roma Tor Vergata, Roma, Italy*
- ³²*Nikhef National Institute for Subatomic Physics, Amsterdam, Netherlands*
- ³³*Nikhef National Institute for Subatomic Physics and VU University Amsterdam, Amsterdam, Netherlands*
- ³⁴*AGH—University of Science and Technology, Faculty of Physics and Applied Computer Science, Kraków, Poland*
- ³⁵*Henryk Niewodniczanski Institute of Nuclear Physics Polish Academy of Sciences, Kraków, Poland*
- ³⁶*National Center for Nuclear Research (NCBJ), Warsaw, Poland*
- ³⁷*Horia Hulubei National Institute of Physics and Nuclear Engineering, Bucharest-Magurele, Romania*
- ³⁸*Petersburg Nuclear Physics Institute NRC Kurchatov Institute (PNPI NRC KI), Gatchina, Russia*
- ³⁹*Institute for Nuclear Research of the Russian Academy of Sciences (INR RAS), Moscow, Russia*
- ⁴⁰*Institute of Nuclear Physics, Moscow State University (SINP MSU), Moscow, Russia*
- ⁴¹*Institute of Theoretical and Experimental Physics NRC Kurchatov Institute (ITEP NRC KI), Moscow, Russia*
- ⁴²*Yandex School of Data Analysis, Moscow, Russia*
- ⁴³*Budker Institute of Nuclear Physics (SB RAS), Novosibirsk, Russia*
- ⁴⁴*Institute for High Energy Physics NRC Kurchatov Institute (IHEP NRC KI), Protvino, Russia, Protvino, Russia*
- ⁴⁵*ICCUB, Universitat de Barcelona, Barcelona, Spain*
- ⁴⁶*Instituto Galego de Física de Altas Enerxías (IGFAE), Universidade de Santiago de Compostela, Santiago de Compostela, Spain*
- ⁴⁷*Instituto de Física Corpuscular, Centro Mixto Universidad de Valencia—CSIC, Valencia, Spain*
- ⁴⁸*European Organization for Nuclear Research (CERN), Geneva, Switzerland*
- ⁴⁹*Institute of Physics, Ecole Polytechnique Fédérale de Lausanne (EPFL), Lausanne, Switzerland*
- ⁵⁰*Physik-Institut, Universität Zürich, Zürich, Switzerland*
- ⁵¹*NSC Kharkiv Institute of Physics and Technology (NSC KIPT), Kharkiv, Ukraine*
- ⁵²*Institute for Nuclear Research of the National Academy of Sciences (KINR), Kyiv, Ukraine*
- ⁵³*University of Birmingham, Birmingham, United Kingdom*
- ⁵⁴*H.H. Wills Physics Laboratory, University of Bristol, Bristol, United Kingdom*
- ⁵⁵*Cavendish Laboratory, University of Cambridge, Cambridge, United Kingdom*
- ⁵⁶*Department of Physics, University of Warwick, Coventry, United Kingdom*
- ⁵⁷*STFC Rutherford Appleton Laboratory, Didcot, United Kingdom*
- ⁵⁸*School of Physics and Astronomy, University of Edinburgh, Edinburgh, United Kingdom*
- ⁵⁹*School of Physics and Astronomy, University of Glasgow, Glasgow, United Kingdom*

⁶⁰*Oliver Lodge Laboratory, University of Liverpool, Liverpool, United Kingdom*⁶¹*Imperial College London, London, United Kingdom*⁶²*Department of Physics and Astronomy, University of Manchester, Manchester, United Kingdom*⁶³*Department of Physics, University of Oxford, Oxford, United Kingdom*⁶⁴*Massachusetts Institute of Technology, Cambridge, MA, United States*⁶⁵*University of Cincinnati, Cincinnati, OH, United States*⁶⁶*University of Maryland, College Park, MD, United States*⁶⁷*Los Alamos National Laboratory (LANL), Los Alamos, United States*⁶⁸*Syracuse University, Syracuse, NY, United States*⁶⁹*School of Physics and Astronomy, Monash University, Melbourne, Australia (associated with Department of Physics, University of Warwick, Coventry, United Kingdom)*⁷⁰*Pontifícia Universidade Católica do Rio de Janeiro (PUC-Rio), Rio de Janeiro, Brazil**(associated with Universidade Federal do Rio de Janeiro (UFRJ), Rio de Janeiro, Brazil)*⁷¹*Physics and Micro Electronic College, Hunan University, Changsha City, China**(associated with Institute of Particle Physics, Central China Normal University, Wuhan, Hubei, China)*⁷²*Guangdong Provincial Key Laboratory of Nuclear Science, Guangdong-Hong Kong Joint Laboratory of Quantum Matter, Institute of Quantum Matter, South China Normal University, Guangzhou, China**(associated with Center for High Energy Physics, Tsinghua University, Beijing, China)*⁷³*School of Physics and Technology, Wuhan University, Wuhan, China (associated with Center for High Energy Physics, Tsinghua University, Beijing, China)*⁷⁴*Departamento de Fisica, Universidad Nacional de Colombia, Bogota, Colombia (associated with LPNHE, Sorbonne Université, Paris Diderot Sorbonne Paris Cité, CNRS/IN2P3, Paris, France)*⁷⁵*Universität Bonn—Helmholtz-Institut für Strahlen und Kernphysik, Bonn, Germany (associated with Physikalisches Institut, Ruprecht-Karls-Universität Heidelberg, Heidelberg, Germany)*⁷⁶*Institut für Physik, Universität Rostock, Rostock, Germany (associated with Physikalisches Institut, Ruprecht-Karls-Universität Heidelberg, Heidelberg, Germany)*⁷⁷*Eotvos Lorand University, Budapest, Hungary (associated with European Organization for Nuclear Research (CERN), Geneva, Switzerland)*⁷⁸*INFN Sezione di Perugia, Perugia, Italy (associated with INFN Sezione di Ferrara, Ferrara, Italy)*⁷⁹*Van Swinderen Institute, University of Groningen, Groningen, Netherlands**(associated with Nikhef National Institute for Subatomic Physics, Amsterdam, Netherlands)*⁸⁰*Universiteit Maastricht, Maastricht, Netherlands (associated with Nikhef National Institute for Subatomic Physics, Amsterdam, Netherlands)*⁸¹*National Research Centre Kurchatov Institute, Moscow, Russia (associated with Institute of Theoretical and Experimental Physics NRC Kurchatov Institute (ITEP NRC KI), Moscow, Russia)*⁸²*National Research University Higher School of Economics, Moscow, Russia**(associated with Yandex School of Data Analysis, Moscow, Russia)*⁸³*National University of Science and Technology “MISIS”, Moscow, Russia (associated with Institute of Theoretical and Experimental Physics NRC Kurchatov Institute (ITEP NRC KI), Moscow, Russia)*⁸⁴*National Research Tomsk Polytechnic University, Tomsk, Russia (associated with Institute of Theoretical and Experimental Physics NRC Kurchatov Institute (ITEP NRC KI), Moscow, Russia)*⁸⁵*DS4DS, La Salle, Universitat Ramon Llull, Barcelona, Spain (associated with ICCUB, Universitat de Barcelona, Barcelona, Spain)*⁸⁶*University of Michigan, Ann Arbor, United States (associated with Syracuse University, Syracuse, NY, United States)*^aAlso at Università di Genova, Genova, Italy.^bAlso at Università di Modena e Reggio Emilia, Modena, Italy.^cAlso at Università di Ferrara, Ferrara, Italy.^dAlso at Università di Milano Bicocca, Milano, Italy.^eAlso at Università di Bologna, Bologna, Italy.^fAlso at Università di Bari, Bari, Italy.^gAlso at Università di Cagliari, Cagliari, Italy.^hAlso at Novosibirsk State University, Novosibirsk, Russia.ⁱAlso at Department of Physics and Astronomy, Uppsala University, Uppsala, Sweden.^jAlso at Università di Roma Tor Vergata, Roma, Italy.^kAlso at Universidade Federal do Triângulo Mineiro (UFTM), Uberaba-MG, Brazil.^lAlso at Hangzhou Institute for Advanced Study, UCAS, Hangzhou, China.^mAlso at AGH—University of Science and Technology, Faculty of Computer Science, Electronics and Telecommunications, Kraków, Poland.ⁿAlso at Università di Siena, Siena, Italy.^oAlso at Università di Padova, Padova, Italy.

^pAlso at Scuola Normale Superiore, Pisa, Italy.

^qAlso at Università degli Studi di Milano, Milano, Italy.

^rAlso at MSU—Iligan Institute of Technology (MSU-IIT), Iligan, Philippines.

^sAlso at Università di Firenze, Firenze, Italy.

^tAlso at Hanoi University of Science, Hanoi, Vietnam.

^uAlso at P.N. Lebedev Physical Institute, Russian Academy of Science (LPI RAS), Moscow, Russia.

^vAlso at Università di Pisa, Pisa, Italy.

^wAlso at Università della Basilicata, Potenza, Italy.

^xAlso at Università di Urbino, Urbino, Italy.